Research Article

Randomness and Topological Invariants in Pentagonal Tiling Spaces

Juan García Escudero

Facultad de Ciencias, Universidad de Oviedo, 33007 Oviedo, Spain

Correspondence should be addressed to Juan García Escudero, jjge@uniovi.es

We analyze substitution tiling spaces with fivefold symmetry. In the substitution process, the introduction of randomness can be done by means of two methods which may be combined: composition of inflation rules for a given prototile set and tile rearrangements. The configurational entropy of the random substitution process is computed in the case of prototile subdivision followed by tile rearrangement. When aperiodic tilings are studied from the point of view of dynamical systems, rather than treating a single one, a collection of them is considered. Tiling spaces are defined for deterministic substitutions, which can be seen as the set of tilings that locally look like translates of a given tiling. Čech cohomology groups are the simplest topological invariants of such spaces. The cohomologies of two deterministic pentagonal tiling spaces are studied.

1. Introduction

Aperiodic tilings of the plane appeared in the literature in the works of Wang [1] and Penrose [2]. Substitution tilings with noncrystallographic planar symmetries have been intensively studied in the last decades, mainly since the discovery of quasicrystals. The structures are meaningful in several areas like the study of quasicrystalline materials and artificially fabricated macroscopic structures that can be used as photonic or phononic devices.

A property of quasicrystal structures is the appearance of sharp peaks in their diffraction patterns and recent results in this direction use methods familiar from statistical mechanics and from the long-range aperiodic order of tilings [3]. A suitable approach is to work with translation invariant families of mathematical quasicrystals, instead of dealing with a single one. The action of the dynamical systems, which is usually on time, is now translation on space. For recent advances in the mathematics of diffraction in the context of dynamical systems and stochastic spatial point processes, see [4]. On the other hand,

the atoms in a material modeled with a quasicrystal tiling are distributed in such a way that they determine a quasiperiodic potential. The spectrum of the associated Schrödinger Hamiltonian has infinitely many gaps, and its distribution is related to the integer Čech cohomology of the corresponding space of tilings [5, 6]. Other questions tied to the Čech cohomology are connected to the derivation of the internal structure of a material from diffraction data or the type of deformations of the molecular structure that are consistent with the combinatorics of the molecular bonds [7, 8].

Pentagonal, octagonal, decagonal, and dodecagonal quasicrystalline materials have been found in experiments, and tilings with the corresponding symmetries in the diffraction patterns are candidates of their structural models. In this paper, we first study the derivation of both deterministic and random tilings and then we discuss the cohomology groups of some tilings generated by an inflation process. In Section 2, we review a general geometric construction for substitutions and we show how it is applied to the case $d = 5$. Then we analyze the introduction of randomness in the tilings generation and we compute the configurational entropy for certain cases. To conclude, we consider tiling spaces and we study the cohomology groups of the deterministic pentagonal patterns in Section 4.

2. The Substitution Tilings

In [9], the authors studied the systems of tangents of the deltoid and derived a method for the construction of substitution tilings for d-fold symmetries, with d being odd and not divisible by 3. They are particular cases of subsystems of lines included in the constructions described below and in [10, 11]. By a system of lines, we mean a set of d straight lines (d-system) appearing in d orientations. In what follows, $E(n)$ denotes the integer part of n and $s_v \equiv \sin(v\pi/d)$. The following sets of lines in the xy plane define for each d, up to mirror images, finite patterns made with triangles having edge lengths s_v. The patterns contain not only the prototiles but also, when arrows are added as explained below, the first inflation step (level-1 supertiles) and therefore the necessary information for the derivation of the substitution or inflation rules. For $d = 2m$, $(m = 3, 4, \ldots)$ the systems of lines are formed by $x = 0$, $y = 0$, and

$$y = x \tan\left(\frac{v\pi}{d}\right) + \Gamma_{\alpha(v)}, \tag{2.1}$$

where for $v = 1, 2, \ldots, m - 1$, the index $\alpha(v)$ is defined as $\alpha(v) = v$ ($v = 1, 2, \ldots, E(m/2)$), $\alpha(v) = m - v$ ($v = E(m/2) + 1, \ldots, m - 1$), and $\Gamma_{\alpha(v)}$ is defined as $\Gamma_{\alpha(v)} = -\sum_{k=1}^{\alpha(v)} s_{m+1-2k}$. For $v = m + 1, m + 2, \ldots, d - 1$, we have $\alpha(v) = v - m$ ($v = m + 1, \ldots, m + E(m/2)$), $\alpha(v) = d - v$ ($v = m + E(m/2) + 1, \ldots, d - 1$) and $\Gamma_{\alpha(v)} = \sum_{k=1}^{\alpha(v)} s_{m+1-2k}$.

The inflation factors for simple tilings are $[v]_d = s_v/s_1$, $v = 2, 3, \ldots d$, and composite tilings, where the inflation factors are products of the form $[v]_d[\mu]_d \cdots [\lambda]_d$, can be obtained also; although in order to include all the inflation factors, additional constructions must be used [11]. In Section 3, we will study the case $d = 5$ which may be generated with the constructions considered in this section.

In general, arrows must be added to the triangle edges in order to generate tilings by means of substitution rules. The arrows are not necessary for the $d = 2m$ tilings with inflation factors s_m/s_1 because the edge substitution rules are palindrome [10, 11]. A $2d$-system contains a d-system inheriting a structure on each edge. The d-system prototile edges appear subdivided into two segments. We adopt the criterion of assigning an arrow in
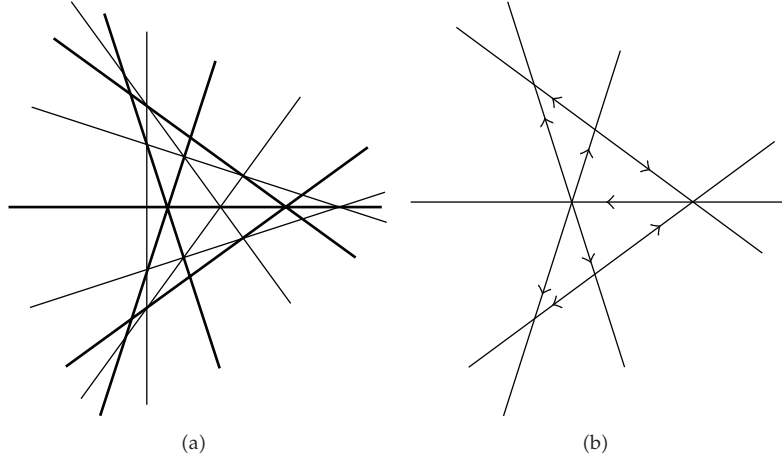
(a)   (b)

Figure 1: System of lines for $d = 5, 10$ (a) and induced arrows for $d = 5$ (b).

the direction going from the longest to the shortest segment, and no arrow when the edge has a barycentric subdivision. When the tiles are juxtaposed along an edge, the arrows on the edge match.

The system of lines for $d = 10$ are (Figure 1)

$$x = 0, \qquad y = 0,$$

$$y = x \tan\left(\frac{\pi}{10}\right) - s_4, \qquad y = x \tan\left(\frac{2\pi}{10}\right) - s_4 + s_2,$$

$$y = x \tan\left(\frac{3\pi}{10}\right) - s_4 + s_2, \qquad y = x \tan\left(\frac{4\pi}{10}\right) - s_4,$$

$$y = x \tan\left(\frac{6\pi}{10}\right) + s_4, \qquad y = x \tan\left(\frac{7\pi}{10}\right) + s_4 + s_2, \tag{2.2}$$

$$y = x \tan\left(\frac{8\pi}{10}\right) + s_4 + s_2, \qquad y = x \tan\left(\frac{9\pi}{10}\right) + s_4.$$

This 10-system contains the subsystem (thick lines in **Figure 1**)

$$x = 0,$$

$$y = x \tan\left(\frac{2\pi}{10}\right) - s_4 + s_2, \qquad y = x \tan\left(\frac{4\pi}{10}\right) - s_4, \tag{2.3}$$

$$y = x \tan\left(\frac{6\pi}{10}\right) + s_4, \qquad y = x \tan\left(\frac{8\pi}{10}\right) + s_4 + s_2,$$

corresponding to $d = 5$. The lines of the 10-system intersect the 5-system on points that determine the arrow directions (**Figure 1(b)**).

The 2D tilings can be described in terms of word sequences in D0L-systems as in [12]. A 0L system is a triple $G = \{\Sigma, h, \omega\}$ where $\Sigma = \{x_1, x_2, \ldots, x_n\}$ is an alphabet, h is a finite substitution on Σ into the set of subsets of Σ^*, and $\omega \in \Sigma^*$ is the axiom or starting symbol. G is called a D0L system if $\#(h(x_i)) = 1$, for every $x_i \in \Sigma$, that is to say, there is only one possible substitution for each tile.

Now we consider the tilings generated with the 5-system. The triangular tile $\mathcal{T}_m(x, y, z)$ has edges x, y, z placed anticlockwise, and the index $m \in \mathbf{Z}_{10}$ denotes relative orientation. The letters A_m, B_m represent the prototiles $\mathcal{T}_m(\alpha, \alpha, \beta)$, $\mathcal{T}_m(\alpha, \beta, \beta)$, respectively, where α, β have lengths s_2, s_1, with $s_k \equiv \sin(k\pi/5)$. The tiles of type A then have edges with relative lengths 1, 1, θ, and the tiles of type B have sides θ, θ, 1, where $\theta = s_2/s_1$ is the golden number. The alphabet is $\Sigma = \{A_m, \tilde{A}_m, B_m, \tilde{B}_m, (,)\}$ with $m \in Z_{10}$. It contains two brackets and letters of type X_i and $\tilde{X}_i$ which represent reflected tiles. The set of production rules h for the tiling T_- is (Figure 2(a)):

$$A_m \longmapsto (\Phi_-[A_m]) = \left(B_{m+4} A_{m+6} \tilde{A}_{m+3} \right),$$

$$B_m \longmapsto (\Phi_-[B_m]) = (B_{m+4} A_{m+6}),$$

$$\tilde{A}_m \longmapsto \left(\Phi_-\left[\tilde{A}_m \right] \right) = \left(\tilde{B}_m \tilde{A}_{m+4} A_{m+3} \right),$$

$$\tilde{B}_m \longmapsto \left(\Phi_-\left[\tilde{B}_m \right] \right) = \left(\tilde{A}_m \tilde{B}_{m+6} \right),$$

$$) \longmapsto),$$

$$(\longmapsto (.$$

(2.4)

Any letter representing an oriented tile can be used as axiom. By iterating the production rules applied to an axiom, we get word sequences that describe the tiling growth. We take the axiom A_m for a given m. In the word $(B_{m+4} A_{m+6} \tilde{A}_{m+3})$, if two letters follow one another inside a bracket, the corresponding oriented triangles are glued face to face in a unique way. In the next derivation step, which gives $((\Phi_-[B_{m+4}])(\Phi_-[A_{m+6}])(\Phi_-[\tilde{A}_{m+3}]))$, two oriented triangles represented by consecutive words enclosed by brackets like $\Phi_-[B_{m+4}]$ and $\Phi_-[A_{m+6}]$ are glued face to face and again the prescription is unique.

A different type of tilings T_+ can be generated with substitution rules characterized by $\Phi_+[X_m] = \Phi_-[\tilde{X}_m]$ for all the prototiles represented by $X_m \in \Sigma$ with $\tilde{\tilde{X}}_m = X_m$. Penrose tilings [2, 13] can be obtained also with the same system of lines but the arrowing is changed for some edges (Figure 2(b)). Having in mind the different arrow decorations for the prototiles, the substitution rules for the Penrose pattern can be obtained formally from Φ_- if we make the replacements $A_m \leftrightarrow \tilde{A}_m$. Fragments of T_-, T_+ and Penrose tilings can be seen in Figures 3 and 4.

3. Random Substitutions

Random tiling problems are of interest from a mathematical and also physical point of view. Quasicrystal order may appear even for random tilings, and it is not yet known if deterministic tilings are better candidates than random tilings for the description of materials with noncrystallographic symmetries. A method for the derivation of random substitutions
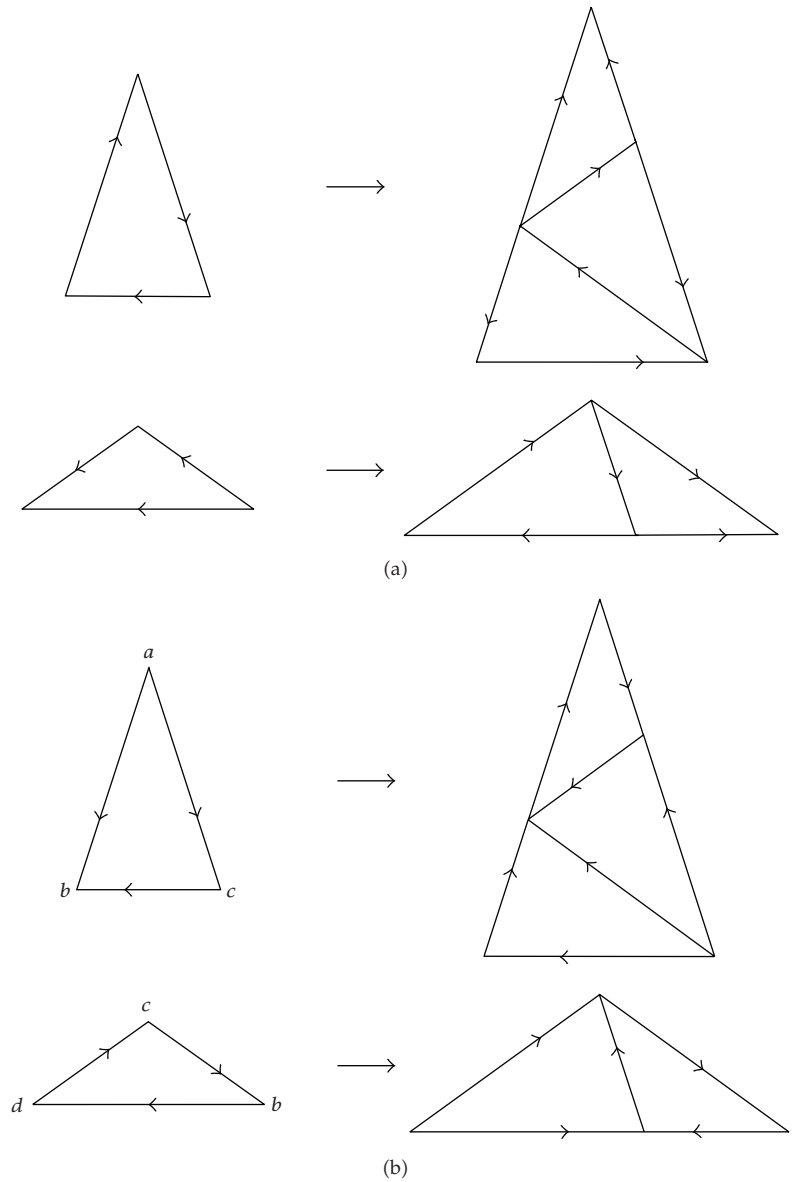
Figure 2: Arrowed prototiles and inflation rules of (a) T_- and (b) Penrose tilings.

with arbitrarily high symmetries has been introduced recently [11]. We analyze two types of nondeterministic tilings, one is related to composition of inflation rules and the other to tile rearrangements.

3.1. Composition of Inflation Rules

The composition of inflation rules $\Phi_-^n \Phi_+^m \Phi_-^k \cdots$ gives tilings that are edge to edge. This is a property that is not in general fulfilled by other random tilings studied in the literature
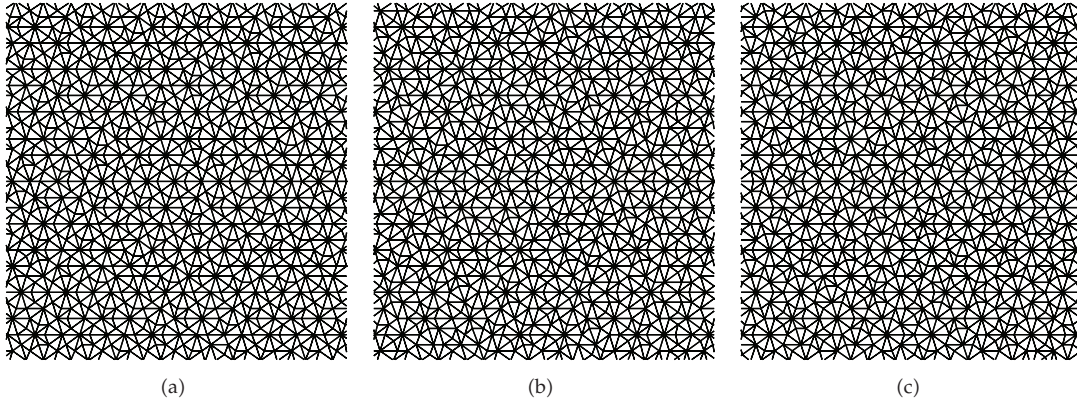
(a)   (b)   (c)

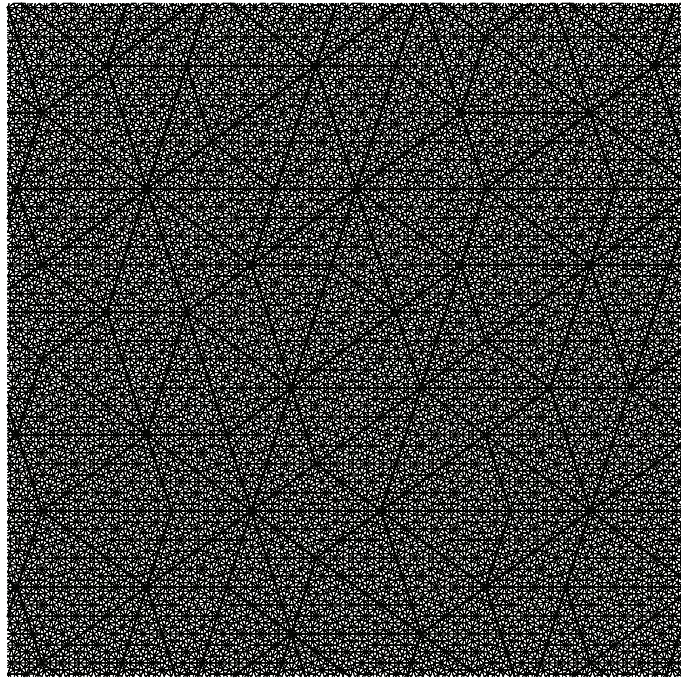**Figure 3:** Fragments of (a) T_-, (b) T_+ and (c) Penrose tilings.

Figure 4: The superposition of $\Phi_+^6[A_1]$ and $\Phi_+^{12}[A_1]$.

[14, 15]. Random substitutions can be described in terms of stochastic L-systems. A stochastic 0L-system is a four-tuple $G_\pi = \{\Sigma, h, \omega, \pi\}$. The alphabet, the set of productions, and the axiom are defined as in a 0L-system. The function $\pi : h \mapsto (0, 1]$, called the probability distribution, maps the set of productions into the set of production probabilities. We define a stochastic DT0L-system as a four-tuple $G_\pi = \{\Sigma, H, \omega, \pi\}$ where H is a set of homomorphisms and $\pi : H \mapsto (0, 1]$. The map is defined for every element in H in contrast to the previous definition where it is defined for every production rule in h. For the case, we are considering $H = \{\Phi_-, \Phi_+\}$ and a fragment of one of the patterns can be seen in Figure 5. New vertex configurations appear which are not present in T_-, T_+ or Penrose tilings.
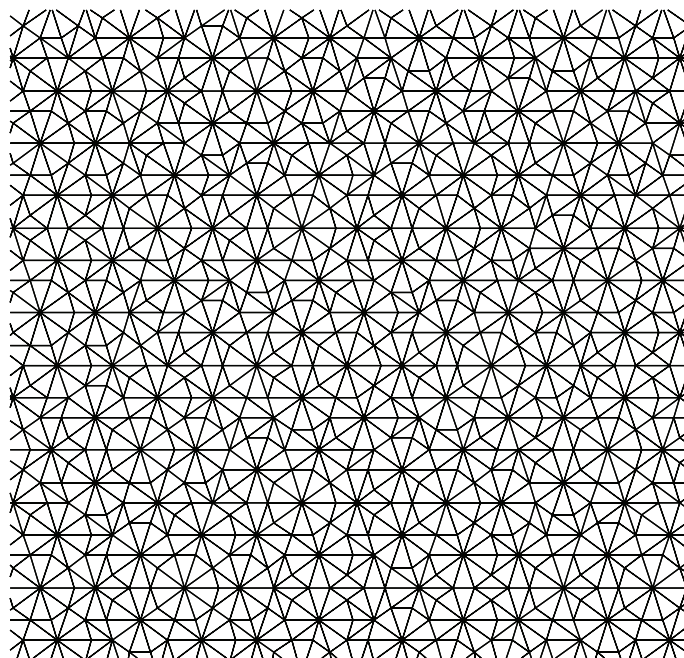
Figure 5: A fragment of $(\Phi_+ \Phi_-)^5$.

3.2. Tile Rearrangements in the Inflation Rules

Another way to get nondeterministic tilings is to introduce tile rearrangements in the inflation rules. First we derive a tiling with the deterministic inflation rules corresponding to an m-system followed by prototile subdivision by the d-system which contains it ($d = 2m, 4m, \ldots$), and then we apply tile rearrangements. In Figure 6(a) we can see the 10-system with possible edge flips forming edges of a pentagon. The tiles corresponding to the 5-system are represented in Figure 6(b). We begin by applying the substitutions Φ_- or Φ_+, and then we get two possibilities for subdivision of one of the tiles and just one for the other (Figure 6(c)).

The configurational entropy S for a sequence of patterns obtained by a random substitution process is defined as the logarithm of the number of patterns of a given size and shape (or level-n supertiles) divided by the number of tiles N_n in the thermodynamic limit

$$\lim_{n \to \infty} \frac{\text{Log} \, \#_n}{N_n}, \tag{3.1}$$

where $\#_n$ is the number of level-n supertiles after applying n times the inflation rules. Now we compute S along the lines of [11] by randomizing T_- or T_+ in two cases: prototile subdivision by $d = 10$ and $d = 20$ followed by tile rearrangements as indicated in Figures 6(b) and 8.
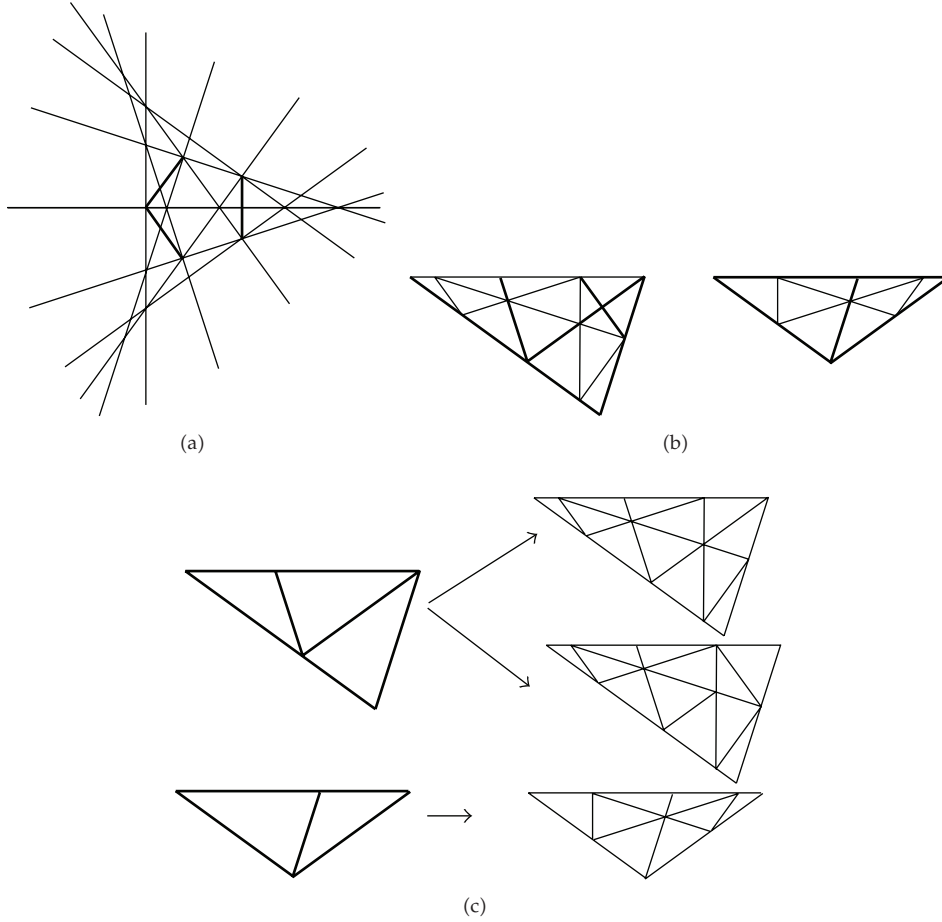
(a)

(b)

(c)

Figure 6: (a) The 10-system with thick lines indicating flipped edges. (b) The first inflation step corresponding to $d = 5$ is indicated by thick lines; prototile subdivision by the 10-system is represented with thin lines and the thicker line indicates the possible tile flip. (c) First inflation step followed by prototile subdivision and the two possibilities of subdividing one of the prototiles.

The frequencies of the tiles $\mathcal{F}_A$, $\mathcal{F}_B$ in the tiling are given by the elements of the normalized eigenvector corresponding to the eigenvalue with largest modulus, or Perron-Frobenius eigenvalue, of the 2D prototile substitution matrix which in this case is

$$\begin{pmatrix} 2 & 1 \\ 1 & 1 \end{pmatrix}. \tag{3.2}$$

The Perron-Frobenius eigenvalue is θ^2 with algebraic conjugate θ^{-2}, and the characteristic polynomial is $x^2 - 3x + 1$. The frequencies are then

$$(\mathcal{F}_A, \mathcal{F}_B) = \left(\theta^{-1}, \theta^{-2}\right). \tag{3.3}$$

The general solution to the difference equation

$$T(n + 2) = 3T(n + 1) + T(n) \tag{3.4}$$

is

$$T(n) = k_1\theta^{2n} + k_2\theta^{-2n}. \tag{3.5}$$

The number of A and B tiles after n iterations is $N_n^A = k_1^A\theta^{2n} + k_2^A\theta^{-2n}$ and $N_n^B = k_1^B\theta^{2n} + k_2^B\theta^{-2n}$, respectively, and the total number of tiles is $N_n = k_1\theta^{2n} + k_2\theta^{-2n}$, where k_i^A, k_i^B, k_i, $i = 1, 2$ are constants determined by the initial conditions about the prototiles content.

The number of patterns after iterating n times (level-n supertiles) is

$$2^{\omega(\Phi(A))N_{n-1}^A + \omega(\Phi(B))N_{n-1}^B}, \tag{3.6}$$

where $\omega(\Phi(X))$ is the number of tile rearrangements in the first inflation step of $X = A, B$. By taking into account

$$\lim_{n \to \infty} \frac{N_{n-1}^x}{N_n} = \frac{1}{\theta^2}\frac{k_1^x}{k_1} = \frac{1}{\theta^2}\mathcal{F}_x, \tag{3.7}$$

we have

$$S = \frac{1}{\theta^2}\sum_X \omega(\Phi(X))\mathcal{F}_X \mathrm{Log}\, 2. \tag{3.8}$$

By examining the case $d = 5$ included in $d = 10$, we get $\omega(\Phi(A)) = 1$, $\omega(\Phi(B)) = 0$, as indicated in Figure, 6(c), therefore,

$$S = \frac{1}{\theta^3}\mathrm{Log}\, 2 \approx 0.16. \tag{3.9}$$

The case $d = 5$ included in $d = 20$ can be seen in Figure 7. We have now $\omega(\Phi(A)) = 5$, $\omega(\Phi(B)) = 3$ (Figure 8) and

$$S = \theta\,\mathrm{Log}\, 2 \approx 1.12. \tag{3.10}$$

If we randomize T_- or T_+ by considering the 5-system included in a d-system with higher d, we can obtain random tilings with increasing entropy values. Also the combination of the two methods discussed in this section is possible, and they give always edge to edge tilings.

The relation between diffuse scattering and randomness has been studied in [4, 16]. By comparing diffraction of point sets ranging from deterministic to fully stochastic, the authors show that diffraction is in some cases insensitive to the degree of order. The following is an open question: what is the role of entropy in the diffraction patterns of the structures described above.
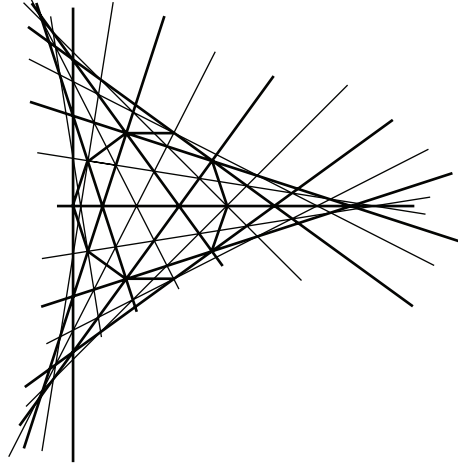
Figure 7: The 20-system with thick lines indicating flipped edges and the $d = 5$ system.
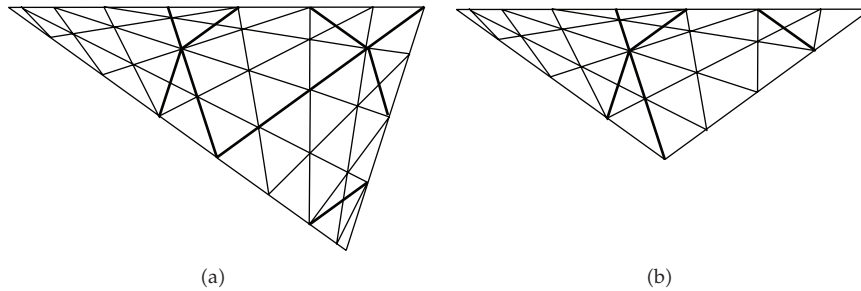

(a)   (b)

Figure 8: Prototile subdivision by the 20-system is represented with thin lines and the thicker line indicates the possible tile flips.

4. Cohomology Groups of the Deterministic Tiling Spaces

A tiling space Ω_T can be seen as the set of tilings that locally look like translates of a tiling T. Anderson and Putnam studied the cohomology of substitution tiling spaces as inverse limits of branched manifolds [17]. They proved that the cohomology can be computed by means of a CW complex Γ_1 on collared tiles which are formed to get a substitution that "forces its border", a concept introduced in [6]. The cell complex Γ_0 contains one copy of every kind of tile that is allowed with some edges identified for the 2D cases, and the result is a branched surface. If somewhere in the tiling, a tile shares an edge with another tile, then those two edges are identified. Tiles labelled by the pattern of their nearest neighbors are called collared tiles, and the cell complex Γ_1 is obtained by stitching one copy of each collared tile. If σ is the map representing the substitution rule, we denote by γ_k ($k = 0, 1$) the map induced on the cell complex Γ_k by σ. A substitution is said to force the border if there is a positive integer n such that any two level-n supertiles of the same type have the same pattern of neighboring tiles. A method for describing an arbitrary substitution tiling space by a substitution that forces the border was introduced in [17]. It is obtained by rewriting the substitution in terms of collared tiles. If $\mathscr{H}^k(\Gamma_1, \mathbf{Z})$ denotes the Čech cohomology with integer coefficients of the complex Γ_1,

then it is shown in [17] that the cohomology $\check{\mathscr{H}}^k(\Omega_\sigma)$ of the tiling space associated with σ is isomorphic to the direct limit of the system of abelian groups

$$\check{\mathscr{H}}^k(\Gamma_1,\mathbf{Z}) \xrightarrow{\ \ }_{\gamma_1^*} \check{\mathscr{H}}^k(\Gamma_1,\mathbf{Z}) \xrightarrow{\ \ }_{\gamma_1^*} \check{\mathscr{H}}^k(\Gamma_1,\mathbf{Z}) \longrightarrow \cdots = \varinjlim_{\gamma_1^*} \mathscr{H}^k(\Gamma_1,\mathbf{Z}) \tag{4.1}$$

for $k = 0, 1, 2, \ldots$. If the substitution forces its border, then the same conclusions hold replacing Γ_1 and γ_1 by Γ_0 and γ_0.

4.1. Penrose Tiling Space

Now we study the cohomology of Penrose tiling spaces Ω_P along the lines of [8, 18] but with different inflation rules. The rotation group $\mathbf{Z}_{10}$ acts freely on edges and tiles. We have two edges α, γ with length s_2, 2 edges β, δ with length s_1, and four tile types $A = \mathcal{T}(r^5\delta, r^8\gamma, r^7\alpha)$, $B = \mathcal{T}(r^5\gamma, r^9\delta, r\beta)$, $\tilde{A} = \mathcal{T}(\delta, r^8\alpha, r^7\gamma)$, and $\tilde{B} = \mathcal{T}(\gamma, r^4\beta, r^6\delta)$ with $r^{10} = 1$ and each appears in 10 orientations. The vertices of A and B can be seen in Figure 2(b), while the vertices of $\tilde{A}$ and $\tilde{B}$ can be obtained by replacing $\{a, b, c\} \mapsto \{b, d, a\}$ and $\{c, d, b\} \mapsto \{d, a, c\}$ on A and B. They satisfy $a = rb$, $b = ra$, $c = rd$, and $d = rc$. The uncollared Anderson-Putnam complex Γ_0 has Euler characteristic $\chi = 4$.

The four irreducible representations of $\mathbf{Z}_{10}$ over the integers are the 1-dimensional scalar ($r = 1$) and pseudoscalar ($r = -1$) representations and two 4-dimensional representations. The vector and the pseudovector representations have r acting by multiplication on the rings $\mathcal{R}_1 = \mathbf{Z}[r]/(r^4 - r^3 + r^2 - r + 1)$ and $\mathcal{R}_2 = \mathbf{Z}[r]/(r^4 + r^3 + r^2 + r + 1)$, respectively. In this case the vertices appear in the scalar and pseudoscalar representations, while the edges and faces appear in all representations. If the cochain groups are denoted by C^k, then, for $k = 0, 1$, the coboundary maps $\delta_k = \partial_{k+1}^T : C^k \mapsto C^{k+1}$ are obtained from the boundary maps:

$$\partial_2 = \begin{pmatrix} r^7 & 0 & -r^8 & 0 \\ 0 & -r & 0 & r^4 \\ -r^8 & -r^5 & r^7 & 1 \\ -r^5 & -r^9 & 1 & r^6 \end{pmatrix} \tag{4.2}$$

in all representations and

$$\partial_1 = \begin{pmatrix} 1-r & 0 & -1 & 1 \\ 0 & r-1 & 1 & -r \end{pmatrix} \tag{4.3}$$

in the scalar and pseudoscalar representations.

Scalar Representation $r = 1$

In the scalar representation, $C^0 = \mathbf{Z}^2$, $C^1 = \mathbf{Z}^4$, $C^2 = \mathbf{Z}^4$. We have rank $\delta_0 = 1$ and rank $\delta_1 = 2$ and $\mathscr{H}^0 = \text{Ker } \delta_0 = \mathbf{Z}$, $\mathscr{H}^1 = \text{Ker } \delta_1/\text{Im } \delta_0 = \mathbf{Z}$, and $\mathscr{H}^2 = \mathbf{Z}^4/\text{Im } \delta_1 = \mathbf{Z}^2$.
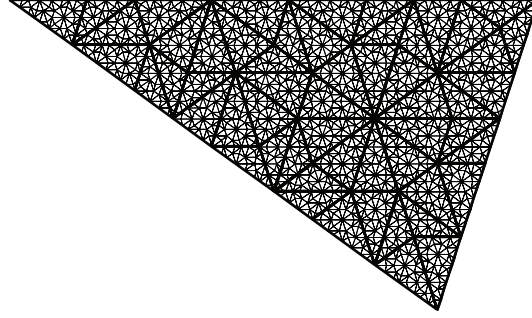
Figure 9: The superposition of $\Phi_P^4[A_1]$ and $\Phi_P^8[A_1]$.

Pseudoscalar Representation $r = -1$

In the pseudoscalar representation, $C^0 = \mathbf{Z}^2$, $C^1 = \mathbf{Z}^4$, and $C^2 = \mathbf{Z}^4$ also. But now both δ_0 and δ_1 have rank 2 and $\mathscr{H}^0 = \mathscr{H}^1 = 0$, $\mathscr{H}^2 = \mathbf{Z}^2$.

Vector Representation

There are no vertices in the vector representation, while C^1, C^2 are free modules of dimensions 4 over the ring $\mathcal{R}_1$. The matrix δ_1 has rank 3 over $\mathcal{R}_1$ and, as abelian groups, we have $\mathscr{H}^1 = \mathscr{H}^2 = \mathbf{Z}^4$.

Pseudovector Representation

In the pseudovector representation, C^1, C^2 are free modules of dimensions 4 over the ring $\mathcal{R}_2$. The map δ_1 is an isomorphism and $\mathscr{H}^0 = \mathscr{H}^1 = \mathscr{H}^2 = 0$.

We have obtained the cohomology of the uncollared complex Γ_0 which is enough because the Penrose tiling forces the border [17], in four steps (Figure 9). To get the cohomology of the tiling space Ω_P, we need to compute the direct limit of the cohomologies under the substitution. But the substitution is invertible and the direct limit of each $\mathscr{H}^k$ is simply $\mathscr{H}^k$. By taking into account all the irreducible representations, we get the well-known result:

$$\check{\mathscr{H}}^0(\Omega_P) = \mathbf{Z}, \qquad \check{\mathscr{H}}^1(\Omega_P) = \mathbf{Z}^5, \qquad \check{\mathscr{H}}^2(\Omega_P) = \mathbf{Z}^8. \tag{4.4}$$

4.2. The Tiling Space Ω_{Ξ_+}

The tiling space Ω_{Ξ_+} is associated with Φ_+ described in Section 2. Iteration of the inflation rules shows that the tiles appear in 5 different orientations. We modify the inflation rules in such a way that, in any inflation step, the prototiles appear in the same 5 orientations (Figure 10). The possible vertex configurations can be seen in Figure 11. The analysis of level-6 supertiles shows that the substitution forces the border. In fact, the level-6 superedges with relative length s_2 have the following pattern of vertex configurations (Figure 12)

$$5327329253273292532925, \tag{4.5}$$
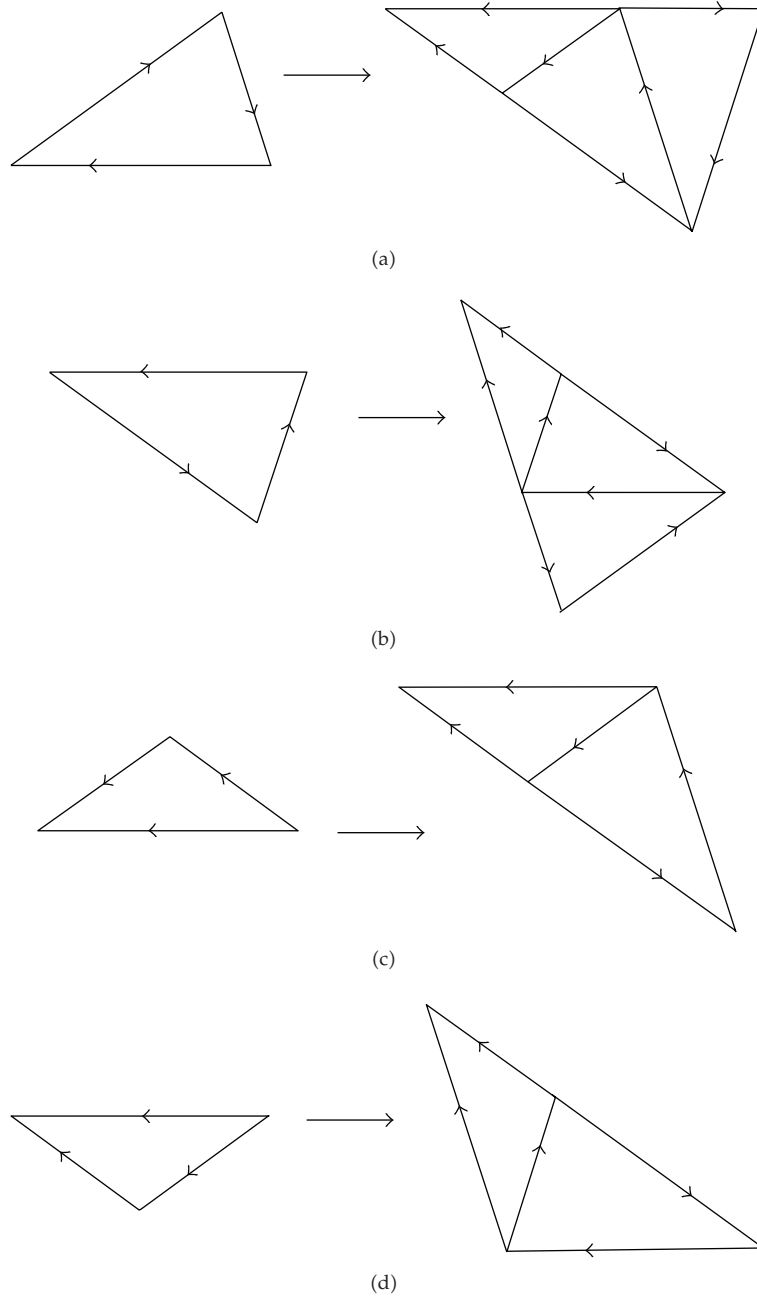
(a)

(b)

(c)

(d)

Figure 10: The inflation rules for the tiling space Ω_{Ξ_+}.

and the sequence of vertices in the superedges with relative length s_1 is
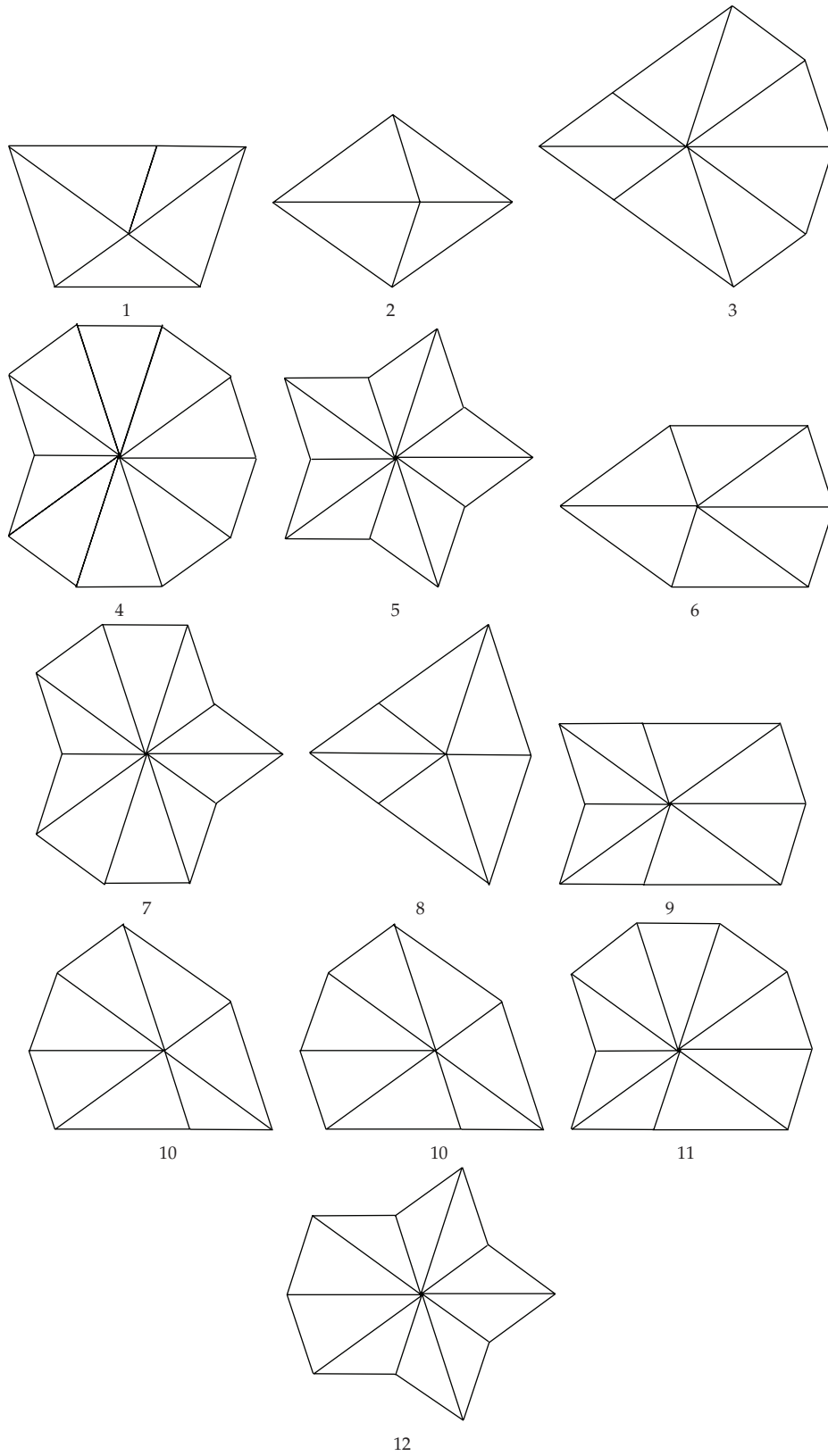
$$53273292532925 \qquad (4.6)$$
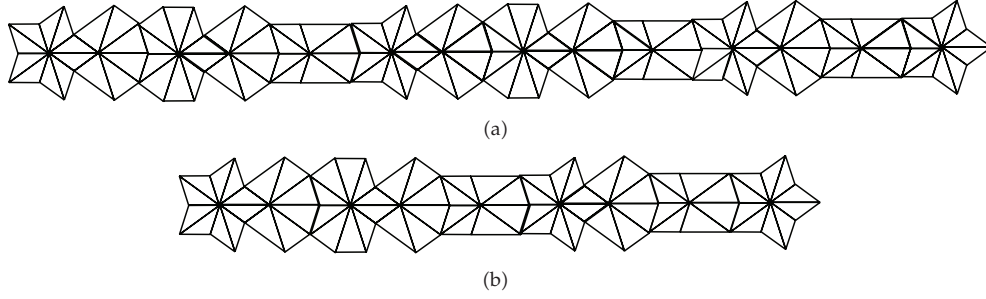
Figure 11: Atlas of vertex configurations of T_+.

(a)

(b)

Figure 12: Vertex sequences in the level-6 superedges of types α (a) and β (b) in T_+.

Therefore, it is enough to consider, up to rotation, 2 edges α, β with lengths s_2, s_1, respectively, and 4 tiles: $A = \mathcal{T}(r^2\alpha, \beta, \alpha)$, $B = \mathcal{T}(r^2\alpha, r^4\alpha, r^2\beta)$, $C = \mathcal{T}(r^2\alpha, r^3\beta, r^4\beta)$, and $D = \mathcal{T}(r^2\alpha, r^3\beta, r^4\beta)$ with $r^5 = 1$. The substitution rules, with $m \in \mathbf{Z}_5$, are (Figure 10)

$$
\begin{aligned}
A_m &\longmapsto (D_m B_{m+2} A_{m+1}), \\
B_m &\longmapsto (C_{m+4} A_{m+2} B_{m+3}), \\
C_m &\longmapsto (D_m B_{m+2}), \\
D_m &\longmapsto (C_{m+4} A_{m+2}), \\
) &\longmapsto), \\
(&\longmapsto .(
\end{aligned}
\tag{4.7}
$$

The rotation group $\mathbf{Z}_5$ acts freely on edges and tiles. We have four tile types and two edges, each in five orientations. All the vertices are identified to one vertex a with $a = ra$. A different case with the same property is the Ammann-Beenker octagonal tiling [19]. The Anderson-Putnam complex Γ_0 of Ω_{Ξ_+} has Euler characteristic $\chi = 11$.

The two irreducible representations of $\mathbf{Z}_5$ over the integers are the 1-dimensional scalar ($r = 1$) representation and the 4-dimensional vector representation which has r acting by multiplication on the ring $\mathbf{Z}[r]/(r^4 + r^3 + r^2 + r + 1)$. The vertex appears only in the scalar representation, while the edges and faces appear in all representations. For $k = 0, 1$, the coboundary maps $\delta_k = \partial_{k+1}^T : C^k \mapsto C^{k+1}$ are deduced from the boundary maps:

$$
\partial_2 = \begin{pmatrix} -r^2 - 1 & r^2 + r^4 & -r^2 & r^2 \\ -1 & r^2 & r^3 + r^4 & -r^3 - r^4 \end{pmatrix}
\tag{4.8}
$$

and $\partial_1 = 0$.

Scalar Representation $r = 1$

In the scalar representation, the cochain groups are $C^0 = \mathbf{Z}$, $C^1 = \mathbf{Z}^2$, and $C^2 = \mathbf{Z}^4$. The rank of δ_1 is 2, and then we have $\mathcal{H}^0 = \text{Ker } \delta_0 = \mathbf{Z}$, $\mathcal{H}^1 = \text{Ker } \delta_1/\text{Im } \delta_0 = 0$, and $\mathcal{H}^2 = \mathbf{Z}^4/\text{Im } \delta_1 = \mathbf{Z}^2$.

Now we look at the direct limit of the cohomologies. The substitution acts as the identity on the vertex a. The substitution matrix on 2-chains is, according to (4.7),

$$\sigma_2 = \begin{pmatrix} r & r^2 & 0 & r^2 \\ r^2 & r^3 & r^2 & 0 \\ 0 & r^4 & 0 & r^4 \\ 1 & 0 & 1 & 0 \end{pmatrix}, \tag{4.9}$$

while the matrix on 1-chains is

$$\sigma_1 = \begin{pmatrix} r^2 & r^3 \\ r & 0 \end{pmatrix}. \tag{4.10}$$

The induced matrix on 2-cochains is $\sigma_2^* = \sigma_2^T$ which is an isomorphism, and the direct limit gives a contribution of $\mathbf{Z}^2$ to $\check{\mathscr{H}}^2$.

Vector Representation

In the vector representation, C^0 is trivial while C^1, C^2 are free modules of dimensions 2 and 4 over the ring $\mathcal{R} = \mathbf{Z}[r]/(r^4 + r^3 + r^2 + r + 1)$. The matrix δ_1 has rank 1 over $\mathcal{R}$. In this case, $\mathscr{H}^0 = 0, \mathscr{H}^1$ has one copy of the ring $\mathcal{R}$, and $\mathscr{H}^2$ has three copies of $\mathcal{R}$; therefore, as abelian groups, we have $\mathscr{H}^1 = \mathbf{Z}^4$, $\mathscr{H}^2 = \mathbf{Z}^{12}$. The ranks of σ_1^*, σ_2^* over $\mathcal{R}$ are 2 and 4, respectively, and the direct limit gives a contribution of $\mathbf{Z}^4$ to $\check{\mathscr{H}}^1$ and $\mathbf{Z}^{12}$ to $\check{\mathscr{H}}^2$.

Adding up the contributions of each representation, we get

$$\check{\mathscr{H}}^0(\Omega_{\Xi_+}) = \mathbf{Z}, \qquad \check{\mathscr{H}}^1(\Omega_{\Xi_+}) = \mathbf{Z}^4, \qquad \check{\mathscr{H}}^2(\Omega_{\Xi_+}) = \mathbf{Z}^{14}. \tag{4.11}$$

The group $\check{\mathscr{H}}^1$ has one copy of the vector representation for both Ω_{Ξ_+} and Ω_P and one of the scalar representation only for Ω_P. We also see that $\check{\mathscr{H}}^2$ contains two copies of the scalar representation for both Ω_{Ξ_+} and Ω_P, and the additional terms are two copies of the pseudoscalar representation for Ω_P, while the vector representation gives a contribution of $\mathbf{Z}^4$ for Ω_P and $\mathbf{Z}^{12}$ for Ω_{Ξ_+}. The tiling spaces Ω_T that we consider in this paper are formed by the closure of the translational orbit of one tiling. The finite rotation group $\mathbf{Z}_n$ acts on Ω_T, and the quotient $\Omega_T/\mathbf{Z}_n$ yields the space $\overline{\Omega}_T$ of tilings modulo rotation about the origin [8]. The cohomology of $\overline{\Omega}_T$ is the rotationally invariant part of the cohomology of Ω_T, and we have

$$\check{\mathscr{H}}^0\left(\overline{\Omega}_T\right) = \mathbf{Z}, \qquad \check{\mathscr{H}}^2\left(\overline{\Omega}_T\right) = \mathbf{Z}^2 \tag{4.12}$$

for $T = P, \Xi_+$, but $\check{\mathscr{H}}^1(\overline{\Omega}_P) = \mathbf{Z}$ whereas $\check{\mathscr{H}}^1(\overline{\Omega}_{\Xi_+}) = 0$.
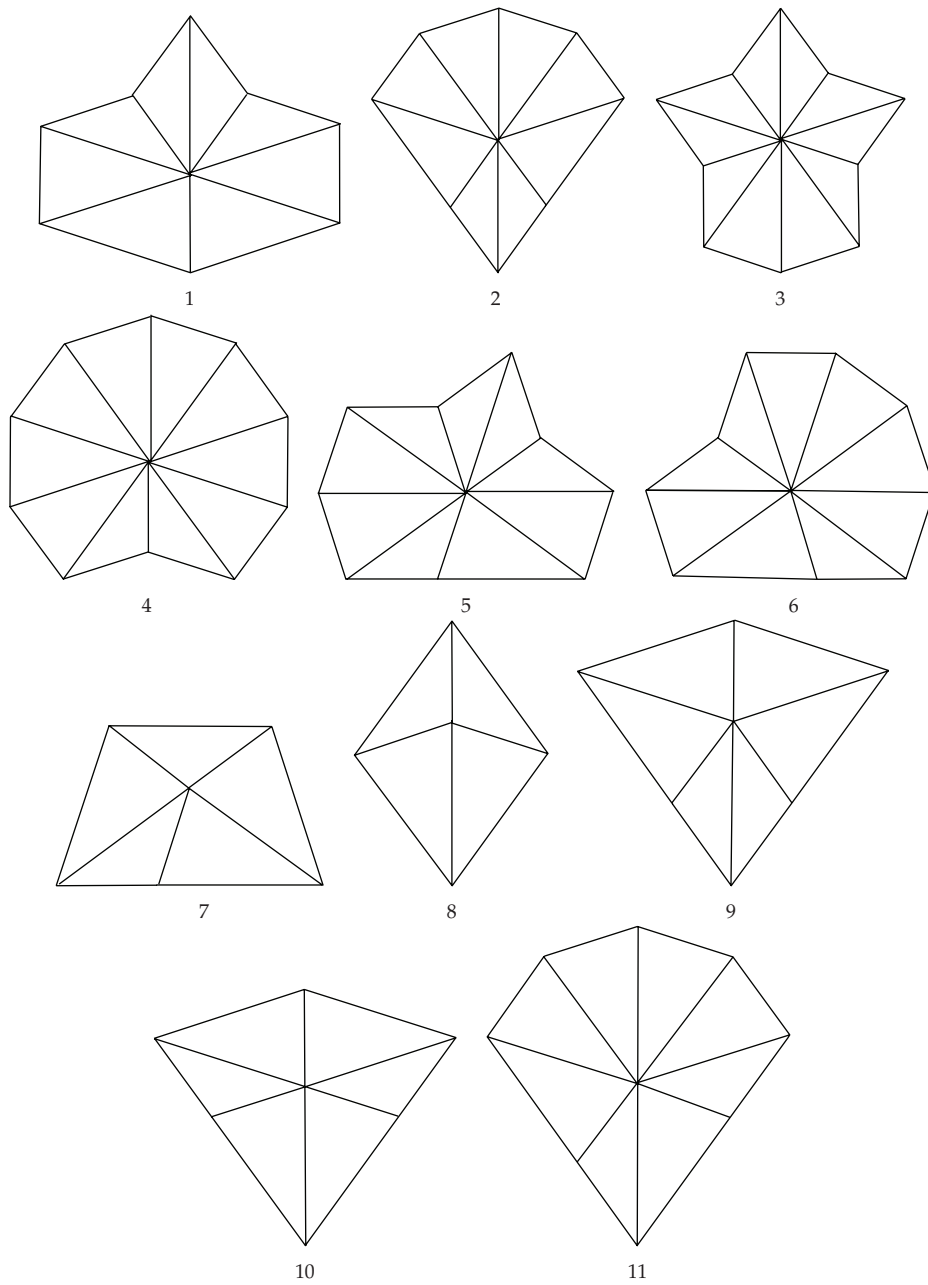
Figure 13: Atlas of vertex configurations of T_-.

4.3. The Tiling Space Ω_{Ξ_-}

In this case, connected with Φ_- in Section 2, the substitution does not force the border and we have to use collared tiles. We have now eight vertices 1, 2, 3, 4, 5, $\tilde{5}$, 6, $\tilde{6}$. In Figure 13, where we have represented the uncollared vertex configurations, the vertices without

bilateral symmetry correspond to 5, $\widetilde{6}$, 7, $\widetilde{11}$. Disregarding the vertices in the borders, there are, in the collared tiles, eight edge types: α, β, γ, $\widetilde{\gamma}$ with length s_2 and δ, η, ϵ, $\widetilde{\epsilon}$ with length s_1 associated with the following vertex sequences (Figure 14) in the level-6 superedges (commas are used when a vertex is represented by two digits):

$$\alpha : (48)^2 2(48)^2 (248)^2 48248,$$

$$\beta : (10,9193)^2 10,93,10,193,10,9,$$

$$\gamma : 11,7675,11,76(75,11)^2 7675,11,7,$$

$$\delta : 84284(842)^2 8,$$

$$\eta : 9,10,3919(10,39)^2,$$

$$\epsilon : 7,11,5767(11,57)^2,$$

(4.13)

and $\widetilde{\gamma}, \widetilde{\epsilon}$ are mirror images of γ, ϵ.

The seven tile types A, B, C, D, E, F, G have edges $A(\epsilon, \gamma, \widetilde{\gamma})$, $B(\eta, \gamma, \beta)$, $C(\epsilon, \gamma, \beta)$, $D(\epsilon, \alpha, \beta)$, $E(\widetilde{\gamma}, \epsilon, \delta)$, $F(\beta, \epsilon, \delta)$, and $G(\widetilde{\gamma}, \epsilon, \epsilon)$, respectively. Observe that with this notation A, B, C, D have Section 2A-shape and E, F, G the B-shape. Now by taking into account the 8 vertices, we have, up to rotation, 86 edges and 106 prototiles. The edges and tiles appear in five different orientations and the complex Γ_1 of Ω_{Ξ_-} has Euler characteristic $\chi = 108$. The inflation rules for the prototiles, up to mirror reflection, can be seen in Table 1, where each letter representing a tile type is followed by their vertices and by the prototiles that appear in the substitution rules. In Figure 15, it is shown a fragment of a pattern obtained by assigning colors to the collared prototiles. We have treated this case without the use of representations, along the lines of [17] (see also [20] for recent results applicable when the tiling does not force the border). The matrices are to large to list here but may be read off from Table 1. The cochain groups are $C^0 = \mathbf{Z}^8$, $C^1 = \mathbf{Z}^{430}$, and $C^2 = \mathbf{Z}^{530}$. The ranks of δ_0, δ_1 are 7 and 419, respectively and $\mathcal{H}^0 = \mathrm{Ker}\,\delta_0 = \mathbf{Z}$, $\mathcal{H}^1 = \mathrm{Ker}\,\delta_1 / \mathrm{Im}\,\delta_0 = \mathbf{Z}^4$, and $\mathcal{H}^2 = \mathbf{Z}^{530} / \mathrm{Im}\,\delta_1 = \mathbf{Z}^{111}$.

The substitution matrix on vertices is

$$\sigma_0 = \begin{pmatrix} 0 & 1 & 0 & 0 & 0 & 0 & 0 & 0 \\ 1 & 0 & 0 & 0 & 0 & 0 & 0 & 0 \\ 0 & 0 & 0 & 1 & 0 & 0 & 0 & 0 \\ 0 & 0 & 1 & 0 & 0 & 0 & 0 & 0 \\ 0 & 0 & 0 & 0 & 0 & 0 & 0 & 1 \\ 0 & 0 & 0 & 0 & 0 & 0 & 1 & 0 \\ 0 & 0 & 0 & 0 & 0 & 1 & 0 & 0 \\ 0 & 0 & 0 & 0 & 1 & 0 & 0 & 0 \end{pmatrix}$$

(4.14)

with $\sigma_0^2 = 1$.

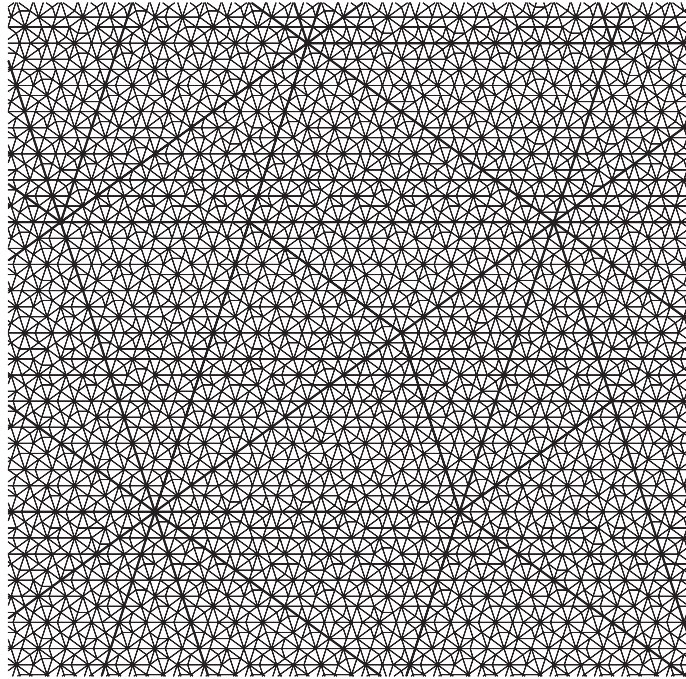**Figure 14:** The superposition of $\Phi_-^6[A_1]$ and $\Phi_-^{12}[A_1]$.

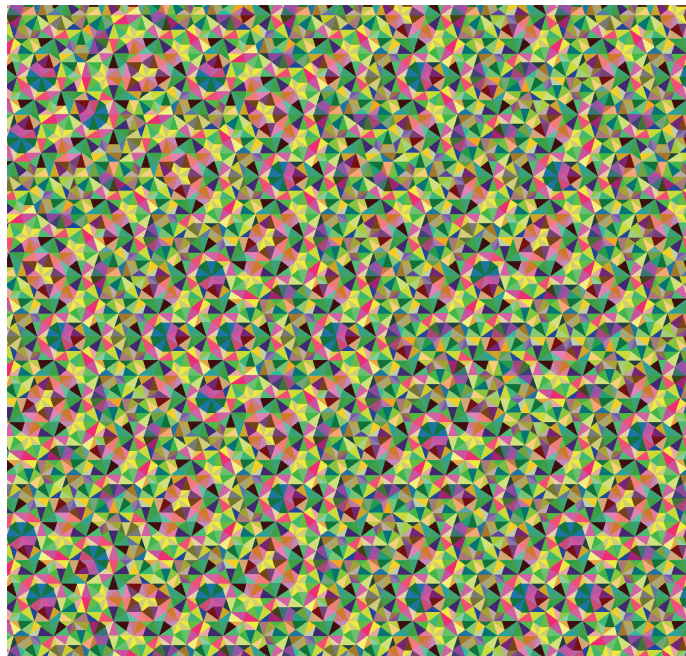**Figure 15:** Fragment of a pattern obtained by assigning colors to the collared tiles, after iteration of the inflation rules in Table 1 for Ω_{Ξ_-}.

We now denote the edges by ω_{xy} if the edge type ω has vertices x, y on its border and $\partial_1\omega_{xy} = y - x$. If $\phi(x)$ represents the image of the vertex x under substitution, then the edge inflation rules are

$$
\begin{aligned}
\alpha_{xy} &\longmapsto \beta_{3\phi(y)}r^3\eta_{3\phi(x)}, & \beta_{xy} &\longmapsto \alpha_{2\phi(y)}r^3\delta_{2\phi(x)}, \\
\gamma_{xy} &\longmapsto \widetilde{\gamma}_{\widetilde{5}\phi(y)}r^3\widetilde{\epsilon}_{\widetilde{5}\phi(x)}, & \widetilde{\gamma}_{xy} &\longmapsto \gamma_{5\phi(y)}r^3\epsilon_{5\phi(x)}, \\
\delta_{xy} &\longmapsto r^2\beta_{\phi(y)\phi(x)}, & \eta_{xy} &\longmapsto r^2\alpha_{\phi(y)\phi(x)}, \\
\epsilon_{xy} &\longmapsto r^2\widetilde{\gamma}_{\phi(y)\phi(x)}, & \widetilde{\epsilon}_{xy} &\longmapsto r^2\gamma_{\phi(y)\phi(x)}.
\end{aligned}
\tag{4.15}
$$

The substitution matrices for the edges and tiles and the corresponding induced matrices on cochains σ_1^*, σ_2^* can be obtained from Table 1 having in mind the relative orientations given by the following rules:

$$
\begin{aligned}
A &\longmapsto r^2Gr^3Cr^4\widetilde{C}, & B &\longmapsto r^2Er^3Dr^4\widetilde{D}, & C &\longmapsto r^2Er^3Dr^4\widetilde{C}, & D &\longmapsto r^2Fr^3Dr^4\widetilde{B}, \\
E &\longmapsto r^2Gr^3C, & F &\longmapsto r^2Er^3D, & G &\longmapsto r^2Gr^3A, \\
\widetilde{A} &\longmapsto \widetilde{G}r^2\widetilde{C}rC, & \widetilde{B} &\longmapsto \widetilde{E}r^2\widetilde{D}rD, & \widetilde{C} &\longmapsto \widetilde{E}r^2\widetilde{D}rC, & \widetilde{D} &\longmapsto \widetilde{F}r^2\widetilde{D}rB, \\
\widetilde{E} &\longmapsto r^3\widetilde{G}\widetilde{C}, & \widetilde{F} &\longmapsto r^3\widetilde{E}\widetilde{D}, & \widetilde{G} &\longmapsto r^3\widetilde{G}\widetilde{A}.
\end{aligned}
\tag{4.16}
$$

The map σ_1^* preserves the quotient $\operatorname{Ker}\delta_1/\operatorname{Im}\delta_0$, while the direct limit of $\mathscr{H}^2$ under σ_2^* is isomorphic to $\mathbf{Z}^{290}/\mathbf{Z}^{229}$, and hence the cohomology groups of the tiling space are

$$
\check{\mathscr{H}}^0(\Omega_{\Xi_-}) = \mathbf{Z}, \qquad \check{\mathscr{H}}^1(\Omega_{\Xi_-}) = \mathbf{Z}^4, \qquad \check{\mathscr{H}}^2(\Omega_{\Xi_-}) = \mathbf{Z}^{61}.
\tag{4.17}
$$

The cohomologies of other tilings significant in quasicrystal research like the Ammann-Beenker tiling spaces Ω_{AB} are well known [19]. Its Anderson-Putnam complex has 1 vertex, 16 edges, and 20 faces with Euler characteristic $\chi = 5$. In this case, $\check{\mathscr{H}}^0(\Omega_{AB}) = \mathbf{Z}$, $\check{\mathscr{H}}^1(\Omega_{AB}) = \mathbf{Z}^5$, $\check{\mathscr{H}}^2(\Omega_{AB}) = \mathbf{Z}^9$. We observe that

$$
\chi = \sum_{m=0}^{2}(-1)^l\operatorname{rank}\left(\check{\mathscr{H}}^m(\Omega_T)\right)
\tag{4.18}
$$

for $T = P, AB, \Xi_+$ but not for Ξ_-.

The integer Čech cohomology of a tiling space is related to the algebraic K-theory. K_0 is the direct sum of the cohomologies of even codimensions, while K_1 is the direct sum of the cohomologies of odd codimension. If a tiling T represents the atoms of a quasicrystal, then the K-theory of Ω_T gives information about the electrical properties of the quasicrystal. The K_0 groups for Ξ_-, Ξ_+ and Penrose tiling spaces are then $\mathbf{Z}\oplus\mathbf{Z}^{61}$, and $\mathbf{Z}\oplus\mathbf{Z}^{14}, \mathbf{Z}\oplus\mathbf{Z}^8$ respectively. There is a trace operator that maps K_0 to $\mathbf{R}$. The image of this map is an additive subgroup of $\mathbf{R}$, called the gap-labeling group of Ω_T, which determines the energy gaps in the spectrum of the Schrödinger operator with a pattern-equivariant potential [5, 19].

Table 1: Prototile contents in the inflation rules for Ω_{Ξ_-}.

$A1 : [1, 5, \tilde{6}] \mapsto G37\ C12\ \tilde{C}13;\ A2 : [\tilde{5}, 5, \tilde{6}] \mapsto G39\ C12\ \tilde{C}13;\ A3 : [\tilde{6}, 5, \tilde{6}] \mapsto G38\ C12\ \tilde{C}13$
$B4 : [2, 1, 3] \mapsto E27\ D22b\ \tilde{D}22a;\ B5 : [4, 1, 3] \mapsto E28\ D22b\ \tilde{D}22a;\ B6a : [6, 1, 3] \mapsto E30b\ D22b\ \tilde{D}22a$
$B6b : [\tilde{6}, 1, 3] \mapsto E30a\ D22b\ \tilde{D}22a;\ C7 : [2, 5, 1] \mapsto E27\ D19\ \tilde{C}8;\ C8 : [2, 6, 5] \mapsto E27\ D25b\ \tilde{C}15$
$C9 : [3, 5, 1] \mapsto E29\ D19\ \tilde{C}8;\ C10 : [4, 5, 1] \mapsto E28\ D19\ \tilde{C}8;\ C11a : [5, 5, 1] \mapsto E31b\ D19\ \tilde{C}8$
$C11b : [\tilde{5}, 5, 1] \mapsto E31a\ D19\ \tilde{C}8;\ C12 : [5, 5, \tilde{5}] \mapsto E31b\ D25a\ \tilde{C}16b;\ C13 : [\tilde{5}, 6, 5] \mapsto E31a\ D25b\ \tilde{C}15$
$C14a : [6, 5, 1] \mapsto E30b\ D19\ \tilde{C}8;\ C14b : [\tilde{6}, 5, 1] \mapsto E30a\ D19\ \tilde{C}8;\ C15 : [6, 5, 5] \mapsto E30b\ D25b\ \tilde{C}16a$
$C16a : [6, 6, 5] \mapsto E30b\ D25b\ \tilde{C}15;\ C16b : [\tilde{6}, 6, 5] \mapsto E30a\ D25b\ \tilde{C}15;\ D17 : [2, 2, 1] \mapsto F32\ D18\ \tilde{B}4$
$D18 : [2, 2, 3] \mapsto F32\ D21\ \tilde{B}5;\ D19 : [2, 2, \tilde{5}] \mapsto F32\ D24a\ \tilde{B}6b;\ D20 : [4, 2, 1] \mapsto F33\ D18\ \tilde{B}4;$
$D21 : [4, 2, 3] \mapsto F33\ D21\ \tilde{B}5;\ D22a : [4, 2, 5] \mapsto F33\ D24b\ \tilde{B}6a;\ D22b : [4, 2, \tilde{5}] \mapsto F33\ D24a\ \tilde{B}6b;$
$D23a : [6, 2, 1] \mapsto F34b\ D18\ \tilde{B}4;\ D23b : [\tilde{6}, 2, 1] \mapsto F34a\ D18\ \tilde{B}4;\ D24a : [6, 2, 3] \mapsto F34b\ D21\ \tilde{B}5$
$D24b : [\tilde{6}, 2, 3] \mapsto F34a\ D21\ \tilde{B}5;\ D25a : [6, 2, \tilde{5}] \mapsto F34b\ D24a\ \tilde{B}6b;\ D25b : [\tilde{6}, 2, \tilde{5}] \mapsto F34a\ D24a\ \tilde{B}6b$
$E26 : [1, 2, 4] \mapsto G35\ C9;\ E27 : [\tilde{5}, 2, 1] \mapsto G36\ C7;\ E28 : [\tilde{5}, 2, 3] \mapsto G36\ C10$
$E29 : [\tilde{5}, 2, 4] \mapsto G36\ C9;\ E30a : [\tilde{5}, 2, 5] \mapsto G36\ C14b;\ E30b : [\tilde{5}, 2, \tilde{5}] \mapsto G36\ C14a$
$E31a : [\tilde{5}, 2, 6] \mapsto G36\ C11b;\ E31b : [\tilde{5}, 2, \tilde{6}] \mapsto G36\ C11a;\ F32 : [3, 2, 1] \mapsto E26\ D17$
$F33 : [3, 2, 3] \mapsto E26\ D20;\ F34a : [3, 2, 5] \mapsto E26\ D23b;\ F34b : [3, 2, \tilde{5}] \mapsto E26\ D23a$
$G35 : [1, 5, 2] \mapsto G40\ A1;\ G36 : [1, 5, 6] \mapsto G40\ A2;\ G37 : [\tilde{5}, 5, 2] \mapsto G42\ A1$
$G38 : [\tilde{5}, 5, 5] \mapsto G42\ A3;\ G39 : [\tilde{5}, 5, 6] \mapsto G42\ A2;\ G40 : [\tilde{6}, 5, 2] \mapsto G41\ A1$
$G41 : [\tilde{6}, 5, 5] \mapsto G41\ A3;\ G42 : [\tilde{6}, 5, 6] \mapsto G41\ A2$

5. Concluding Remarks

Several types of deterministic and random substitutions have been analyzed. We have shown that, apart from the vertex configurations and relative orientations, an essential difference between the spaces of pentagonal tilings Ω_{Ξ_+}, Ω_{Ξ_-} and the very well-known space of Penrose tilings Ω_P is the cohomology, in spite of the fact that the first inflation step in the tiling growth seems to be very similar. Both tiling spaces have finitely generated torsion-free cohomology groups (see [21] for cartesian product tiling spaces related to the constructions in Section 1).

For projection tilings, it has been shown in [22] that in the first cohomology group there is at least a subgroup isomorphic to the reciprocal lattice of the tiling. The minimal dimension of the lattice for an N-fold symmetry tiling in 2D obtained by projection is given by the Eulers totient function $\phi(N)$, which counts the number of positive integers less than N that are coprime to N. For the Penrose tiling $\phi(10) = 4$ and its description by projection can be done with the root-lattice A_4 [23]. As far as the author knows, Ω_{Ξ_+}, Ω_{Ξ_-} have the simplest first cohomology group (and hence K_1-group) of a tiling space in 2D with noncrystallographic symmetries, and its rank coincides with $\phi(5)$. The complexity of the tiling spaces, if measured with the set of (possibly collared) vertex configurations, is reflected in the rank of the second cohomology group and as a consequence in the K_0-group. For certain cases [8], only the rotationally invariant part of the second cohomology group contributes to the gap labeling group, and therefore the Penrose and T_+ tilings have isomorphic groups. However, in contrast to the Penrose tiling, T_+ has a vanishing first cohomology group on the space of tilings modulo a rotation. Another tiling with the same prototiles was derived by the Tübingen group [23]. For a study of its cohomology, which is computationally demanding, see [24].

We have obtained the configurational entropy of sequences of finite patterns generated by particular random substitution processes. In general, the determination of the entropy of the tiling spaces associated to the random tiling ensembles (defined possibly as direct sums of uniquely ergodic spaces) and its physical meaning are open questions.

The constructions studied in Section 2 have been used for the generation of non-periodic ordered tilings in multiconnected flat manifolds. For instance, the d-systems corresponding to $d = 8, 12$ were used in [10] to get random triangulations of the torus and the Klein bottle. In Figure 6(a), it can be seen how a pentagon appears in the modification of the 10-system, the decagon is contained in the 20-system modification (Figure 6) and in general we have an m-gone included in the $2m$-system. This fact can be used to get recursive random simplicial structures for all the closed 2-manifolds, by using two polygons with certain identifications. By considering also higher dimensional manifolds this type of constructions could be of interest in different fields.

Some open problems that should also be considered in the future are the relationship with projection methods, matching rules [25], and the analysis of the topological invariants for both deterministic and random substitution tiling spaces with N-fold symmetries generated with the constructions given in Section 2 and in [11].

Acknowledgment

References

[1] H. Wang, "Proving theorems by pattern recognition-II," *Bell System Technical Journal*, vol. 40, pp. 1–41, 1961.

[2] R. Penrose, "Role of aesthetics in pure and applied research," *Bulletin of the Institute of Mathematics and Its Applications*, vol. 10, article 266ff, 1974.

[3] C. Radin, *Miles of Tiles*, vol. 1 of *Student Mathematical Library*, American Mathematical Society, Providence, RI, USA, 1999.

[4] M. Baake, M. Birkner, and R. V. Moody, "Diffraction of stochastic point sets: explicitly computable examples," *Communications in Mathematical Physics*, vol. 293, no. 3, pp. 611–660, 2010.

[5] J. Bellissard, D. J. L. Herrmann, and M. Zarrouati, "Hulls of aperiodic solids and gap labeling theorems," in *Directions in Mathematical Quasicrystals*, vol. 13 of *CRM Monograph Series*, pp. 207–258, American Mathematical Society, Providence, RI, USA, 2000.

[6] J. Kellendonk, "Noncommutative geometry of tilings and gap labelling," *Reviews in Mathematical Physics*, vol. 7, no. 7, pp. 1133–1180, 1995.

[7] L. Sadun, "Tilings, tiling spaces and topology," *Philosophical Magazine*, vol. 86, no. 6–8, pp. 875–881, 2006.

[8] L. Sadun, *Topology of Tiling Spaces*, vol. 46 of *University Lecture Series*, American Mathematical Society, Providence, RI, USA, 2008.

[9] K.-P. Nischke and L. Danzer, "A construction of inflation rules based on n-fold symmetry," *Discrete & Computational Geometry*, vol. 15, no. 2, pp. 221–236, 1996.

[10] J. G. Escudero, "Random tilings of compact Euclidean 3-manifolds," *Acta Crystallographica. Section A*, vol. 63, no. 5, pp. 391–399, 2007.

[11] J. G. Escudero, "Random tilings of spherical 3-manifolds," *Journal of Geometry and Physics*, vol. 58, no. 11, pp. 1451–1464, 2008.

[12] J. García-Escudero, "Grammars for icosahedral Danzer tilings," *Journal of Physics. A*, vol. 28, no. 18, pp. 5207–5215, 1995.

[13] B. Grünbaum and G. C. Shephard, *Tilings and Patterns*, W. H. Freeman and Company, New York, NY, USA, 1987.

[14] C. Godrèche and J. M. Luck, "Quasiperiodicity and randomness in tilings of the plane," *Journal of Statistical Physics*, vol. 55, no. 1-2, pp. 1–28, 1989.

[15] P. Gummelt, "Generalized substitution rules: concepts and examples," *Zeitschrift fur Kristallographie*, vol. 223, no. 11-12, pp. 805–808, 2008.

[16] M. Baake and U. Grimm, "Kinematic diffraction is insufficient to distinguish order from disorder," *Physical Review B*, vol. 79, no. 2, Article ID 020203, 2009.

[17] J. E. Anderson and I. F. Putnam, "Topological invariants for substitution tilings and their associated *C*-algebras*," *Ergodic Theory and Dynamical Systems*, vol. 18, no. 3, pp. 509–537, 1998.

[18] N. Ormes, C. Radin, and L. Sadun, "A homeomorphism invariant for substitution tiling spaces," *Geometriae Dedicata*, vol. 90, pp. 153–182, 2002.

[19] J. Kellendonk and I. F. Putnam, "Tilings, *C*-algebras, and *K*-theory," in *Directions in Mathematical Quasicrystals*, vol. 13 of *CRM Monograph Series*, pp. 177–206, American Mathematical Society, Providence, RI, USA, 2000.

[20] M. Barge, B. Diamond, J. Hunton, and L. Sadun, "Cohomology of substitution tiling spaces," *Ergodic Theory and Dynamical Systems*, vol. 30, no. 6, pp. 1607–1627, 2010.

[21] J. G. Escudero, "Integer Cech cohomology of a class of n-dimensional substitutions," *Mathematical Methods in the Applied Sciences*, vol. 34, no. 5, pp. 587–594, 2011.

[22] J. Kellendonk and I. F. Putnam, "The Ruelle-Sullivan map for actions of R^n," *Mathematische Annalen*, vol. 334, no. 3, pp. 693–711, 2006.

[23] M. Baake, P. Kramer, M. Schlottmann, and D. Zeidler, "Planar patterns with fivefold symmetry as sections of periodic structures in 4-space," *International Journal of Modern Physics B*, vol. 4, no. 15-16, pp. 2217–2268, 1990.

[24] F. Gähler, J. Hunton, and J. Kellendonk, " Torsion in Tiling Homology and Cohomology," http://arxiv .org/abs/math-ph/0505048.

[25] C. Goodman-Strauss, "Matching rules and substitution tilings," *Annals of Mathematics. Second Series*, vol. 147, no. 1, pp. 181–223, 1998.